Fluctuations of the K/π ratio in nucleus-nucleus collisions: Statistical and transport models

M. I. Gorenstein,[1,2] M. Hauer,[3] V. P. Konchakovski,[2,3] and E. L. Bratkovskaya[1]
[1]*Frankfurt Institute for Advanced Studies, Frankfurt, Germany*
[2]*Bogolyubov Institute for Theoretical Physics, Kiev, Ukraine*
[3]*Helmholtz Research School, University of Frankfurt, Frankfurt, Germany*
(Received 15 December 2008; published 26 February 2009)

Event-by-event fluctuations of the kaon to pion number ratio in nucleus-nucleus collisions are studied within the statistical hadron-resonance gas model (SM) for different statistical ensembles and in the hadron-string-dynamics (HSD) transport approach. We find that the HSD model can qualitatively reproduce the measured excitation function for the K/π ratio fluctuations in central Au + Au (or Pb + Pb) collisions from low Super Proton Synchrotron up to top Relativistic Heavy Ion Collider energies. Substantial differences in the HSD and SM results are found for the fluctuations and correlations of the kaon and pion numbers. These predictions impose a challenge for future experiments.

DOI: 10.1103/PhysRevC.79.024907 PACS number(s): 24.10.Lx, 24.10.Nz, 24.60.Ky, 25.75.Dw

I. INTRODUCTION

The study of event-by-event fluctuations in high-energy nucleus-nucleus ($A + A$) collisions opens new possibilities to investigate the phase transition between hadronic and partonic matter as well as the quantum chromodynamics (QCD) critical point (cf. Ref. [1]). By measuring the fluctuations one might observe anomalies from the onset of deconfinement [2] and dynamical instabilities when the expanding system goes through the first-order transition line between the quark-gluon plasma (QGP) and the hadron gas [3]. Furthermore, the QCD critical point may be signaled by a characteristic pattern in the fluctuations as pointed out in Ref. [4]. However, only recently, due to a rapid development of experimental techniques, first measurements of the event-by-event fluctuations of particle multiplicities [5–8] and transverse momenta [9] in nucleus-nucleus collisions have been performed.

From the theoretical side such event-by-event fluctuations for charged hadron multiplicities (in nucleus-nucleus collisions) have been studied in statistical models [10–19] and in dynamical transport approaches [20–23], which have been used as important tools to investigate high-energy nuclear collisions. We recall that the statistical models reproduce the mean multiplicities of the produced hadrons (see, e.g., Refs. [24–26]), whereas the transport models (see, e.g., Refs. [27–29]) provide, in addition, a dynamical description of the various bulk properties of the system. By studying the various fluctuations within statistical and transport models we have found out that fluctuations provide an extremely sensitive observable—depending on the details of the models—which are partly washed out by looking at general quantities such as ensemble averages.

In particular, there is a qualitative difference in the properties of the mean multiplicity and the scaled variance of the multiplicity distribution in statistical models. In the case of mean multiplicities the results obtained within the grand canonical ensemble (GCE), canonical ensemble (CE), and microcanonical ensemble (MCE) approach each other in the large volume limit. One refers here to the thermodynamical equivalence of the statistical ensembles. However, it was recently found [10,14] that corresponding results for the scaled variances are different in the GCE, CE, and MCE ensembles, and thus the scaled variance is sensitive to global conservation laws obeyed by a statistical system. These differences are preserved in the thermodynamic limit.

Moreover, there is a qualitative difference in the behavior of the scaled variances of multiplicity distributions in statistical and transport models. The transport models predict [21,22] that the scaled variances in central nucleus-nucleus collisions remain close to the corresponding values in proton-proton collisions and increase with collision energy in the same way as the corresponding multiplicities, whereas in the statistical models the scaled variances approach finite values at high collision energy, i.e., become independent of energy. Accordingly, the differences in the scaled variance of charged hadrons can be about factor of 10 at the top RHIC energy [21]. Only upcoming experimental data can clarify the situation.

The QGP stage may form a specific set of primordial fluctuation signals. A well-known example is the equilibrium electric charge fluctuation in QGP that is about a factor 2–3 smaller than in an equilibrium hadron gas [30,31]. To observe primordial QGP fluctuations they should be frozen out during expansion, hadronization, and further hadron-hadron rescatterings. Evolution and survival of the conserved charge fluctuations in systems formed in nucleus-nucleus collisions at the Super Proton Synchrotron (SPS) and Relativistic Heavy Ion Collider (RHIC) energies were discussed in Refs. [32,33]. Note that both the statistical models and the HSD approach used in our study do not include the quark-gluon degrees of freedom. Thus, the fluctuations in the QGP are outside of the scope of the present article.

The measurement of the fluctuations in the kaon-to-pion ratio by the NA49 Collaboration [5] was the first event-by-event measurement in nucleus-nucleus collisions. It was suggested that this ratio might allow us to distinguish the enhanced strangeness production attributed to the QGP phase. Nowadays, the excitation function for this observable is available in a wide range of energies: from the NA49 Collaboration in Pb + Pb collisions at the CERN SPS [7] and from the STAR Collaboration in Au + Au collisions at RHIC [8]. First

statistical model estimates of the K/π fluctuations have been reported in Refs. [34,35], and results from the transport model ultrarelativistic quantum molecular dynamics (UrQMD) in Ref. [36].

In this article we present a systematic study of statistical model results (in different ensembles) in comparison to HSD transport model results for the fluctuations in the kaon to pion number ratio. The article is organized as follows: In Sec. II the characteristic definitions for fluctuations in particle number ratios are introduced. In Sec. III the relevant formulas of the statistical models (in different ensembles) are presented. Statistical and HSD model results for the fluctuations in the kaon-to-pion ratio for central nucleus-nucleus collisions are compared in Sec. IV. In Sec. V the HSD transport model results are additionally confronted with the available data on K/π fluctuations. A summary in Sec. VI closes the article.

II. MEASURES OF PARTICLE RATIO FLUCTUATIONS

A. Notations and approximations

Let us introduce some notations. We define the deviation ΔN_A from the average number $\langle N_A\rangle$ of the particle species A by $N_A = \langle N_A\rangle + \Delta N_A$. Then we define covariance for species A and B

$$\Delta(N_A, N_B) \equiv \langle \Delta N_A \Delta N_B\rangle = \langle N_A N_B\rangle - \langle N_A\rangle\langle N_B\rangle, \tag{1}$$

scaled variance

$$\omega_A \equiv \frac{\Delta(N_A, N_A)}{\langle N_A\rangle} = \frac{\langle(\Delta N_A)^2\rangle}{\langle N_A\rangle} = \frac{\langle N_A^2\rangle - \langle N_A\rangle^2}{\langle N_A\rangle}, \tag{2}$$

and correlation coefficient

$$\rho_{AB} \equiv \frac{\langle \Delta N_A \Delta N_B\rangle}{[\langle(\Delta N_A)^2\rangle\langle(\Delta N_B)^2\rangle]^{1/2}}. \tag{3}$$

The fluctuations of the ratio $R_{AB} \equiv N_A/N_B$ will be characterized by [34,35]

$$\sigma^2 \equiv \frac{\langle(\Delta R_{AB})^2\rangle}{\langle R_{AB}\rangle^2}. \tag{4}$$

Using the expansion,

$$\frac{N_A}{N_B} = \frac{\langle N_A\rangle + \Delta N_A}{\langle N_B\rangle + \Delta N_B} = \frac{\langle N_A\rangle + \Delta N_A}{\langle N_B\rangle} \times \left[1 - \frac{\Delta N_B}{\langle N_B\rangle} + \left(\frac{\Delta N_B}{\langle N_B\rangle}\right)^2 - \cdots\right], \tag{5}$$

one finds to second order in $\Delta N_A/\langle N_A\rangle$ and $\Delta N_B/\langle N_B\rangle$ the average value and the fluctuations of the A to B ratio:

$$\langle R_{AB}\rangle \cong \frac{\langle N_A\rangle}{\langle N_B\rangle}\left[1 + \frac{\omega_B}{\langle N_B\rangle} - \frac{\Delta(N_A, N_B)}{\langle N_A\rangle\langle N_B\rangle}\right], \tag{6}$$

$$\sigma^2 \cong \frac{\Delta(N_A, N_A)}{\langle N_A\rangle^2} + \frac{\Delta(N_B, N_B)}{\langle N_B\rangle^2} - 2\frac{\Delta(N_A, N_B)}{\langle N_A\rangle\langle N_B\rangle} = \frac{\omega_A}{\langle N_A\rangle} + \frac{\omega_B}{\langle N_B\rangle} - 2\rho_{AB}\left[\frac{\omega_A\omega_B}{\langle N_A\rangle\langle N_B\rangle}\right]^{1/2}. \tag{7}$$

If species A and B fluctuate independently according to Poisson distributions (this takes place, for example, in the GCE for an ideal Boltzmann gas) one finds $\omega_A = \omega_B = 1$ and $\rho_{AB} = 0$. Equation (7) then reads

$$\sigma^2 = \frac{1}{\langle N_A\rangle} + \frac{1}{\langle N_B\rangle}. \tag{8}$$

In a thermal gas, the average multiplicities are proportional to the system volume V. Equation (8) demonstrates then a simple dependence of $\sigma^2 \propto 1/V$ on the system volume.

A few examples concerning to Eq. (7) are appropriate here. When $\langle N_B\rangle \gg \langle N_A\rangle$, e.g., $A = K^+ + K^-$ and $B = \pi^+ + \pi^-$, the quantity σ^2 (7) is dominated by the fluctuations of less abundant particles. When $\langle N_A\rangle \cong \langle N_B\rangle$, e.g., $A = \pi^+$ and $B = \pi^-$, the correlation term in Eq. (7) may become especially important. A resonance decaying always into a $\pi^+\pi^-$ pair does not contribute to σ^2 (7) but contributes to the π^+ and π^- average multiplicities. This leads [35] to a suppression of σ^2 (7) in comparison to its value given by Eq. (8). For example, if all π^+ and π^- particles come in pairs from the decay of resonances, one finds the correlation coefficient $\rho_{\pi^+\pi^-} = 1$ in Eq. (7) and thus $\sigma^2 = 0$. In this case, the numbers of π^+ and π^- fluctuate as the number of resonances, but the ratio π^+/π^- does not fluctuate.

B. Mixed-events procedure

The experimental data for N_A/N_B fluctuations are usually presented in terms of the so-called dynamical fluctuations [37][1]

$$\sigma_{\rm dyn} \equiv \mathtt{sign}\left(\sigma^2 - \sigma^2_{\rm mix}\right)\left|\sigma^2 - \sigma^2_{\rm mix}\right|^{1/2}, \tag{9}$$

where σ^2 is defined by Eq. (7) and $\sigma^2_{\rm mix}$ corresponds to the following *mixed-events* procedure.[2] One takes a large number of nucleus-nucleus collision events and measures the numbers of N_A and N_B in each event. Then all A and B particles from all events are combined into one *set*. The construction of *mixed events* is done as follows: One fixes a random number $N = N_A + N_B$ according to the experimental probability distribution $P(N)$, takes randomly N particles (A and/or B) from the *whole set*, fixes the values of N_A and N_B, and returns these N particles into the *set*. This is the mixed event number one. Then one constructs event number 2, number 3, and so on.

Note that the number of events is much larger than the number of hadrons, N, in any single event. Therefore, the probabilities p_A and $p_B = 1 - p_A$, to take the A and B species from the whole *set*, can be considered as constant values during the event construction. Another consequence of a large number of events is the fact that A and B particles in any constructed *mixed event* belong to different *physical events* of nucleus-nucleus collisions. Therefore, the correlations between the N_B and N_A numbers in a physical event are expected to be destroyed in a mixed event. This is the main purpose of the

[1] Other dynamical measures, such as Φ [38,39] and F [35], can be also used.

[2] We describe the idealized mixed-events procedure appropriate for the model analysis. The real experimental mixed-events procedure is more complicated and includes experimental uncertainties, such as particle identification, and so on.

mixed-events construction. For any function $f(N_A, N_B)$ the mixed-events averaging is then defined as

$$\begin{aligned}\langle f(N_A, N_B)\rangle_{\rm mix} &= \sum_N P(N) \sum_{N_A,N_B} f(N_A, N_B)\delta(N - N_A - N_B) \\ &\times \frac{(N_A + N_B)!}{N_A!N_B!} p_A^{N_A} p_B^{N_B}. \end{aligned} \tag{10}$$

The straightforward calculations of mixed averages (10) can be simplified by introducing the generating function $Z(x, y)$,

$$\begin{aligned} Z(x, y) &\equiv \sum_N P(N) \sum_{N_A,N_B} \delta(N - N_A - N_B) \\ &\times \frac{(N_A + N_B)!}{N_A!N_B!} (x p_A)^{N_A} (y p_B)^{N_B} \\ &= \sum_N P(N) \,(x p_A + y p_B)^N \,, \end{aligned} \tag{11}$$

which depends on auxiliary variables x and y. The averages (10) are then expressed as x and y derivatives of $Z(x, y)$ at $x = y = 1$. One finds:

$$\begin{aligned} \langle N_A\rangle_{\rm mix} &= \left(\frac{\partial Z}{\partial x}\right)_{x=y=1} = p_A\langle N\rangle, \\ \langle N_B\rangle_{\rm mix} &= \left(\frac{\partial Z}{\partial y}\right)_{x=y=1} = p_B\langle N\rangle, \end{aligned} \tag{12}$$

$$\begin{aligned} \langle N_A(N_A - 1)\rangle_{\rm mix} &= \left(\frac{\partial^2 Z}{\partial^2 x}\right)_{x=y=1} \\ &= p_A^2\langle N(N - 1)\rangle, \end{aligned} \tag{13}$$

$$\begin{aligned} \langle N_B(N_B - 1)\rangle_{\rm mix} &= \left(\frac{\partial^2 Z}{\partial^2 y}\right)_{x=y=1} \\ &= p_B^2\langle N(N - 1)\rangle, \end{aligned} \tag{14}$$

$$\begin{aligned} \langle N_A N_B\rangle_{\rm mix} - \langle N_A\rangle_{\rm mix}\langle N_B\rangle_{\rm mix} &= \left(\frac{\partial^2 Z}{\partial x \partial y}\right)_{x=y=1} \\ &= p_A p_B\, \omega_N \langle N\rangle, \end{aligned} \tag{15}$$

where

$$\begin{aligned} \langle N\rangle &\equiv \sum_N N P(N), \langle N^2\rangle \equiv \sum_N N^2 P(N), \\ \omega_N &\equiv \frac{\langle N^2\rangle - \langle N\rangle^2}{\langle N\rangle}. \end{aligned} \tag{16}$$

Calculating the N_A/N_B fluctuations for mixed events according to Eq. (7) one gets:

$$\begin{aligned} \sigma^2_{\rm mix} &\equiv \frac{\Delta_{\rm mix}(N_A, N_A)}{\langle N_A\rangle^2} + \frac{\Delta_{\rm mix}(N_B, N_B)}{\langle N_B\rangle^2} - 2\frac{\Delta_{\rm mix}(N_A, N_B)}{\langle N_A\rangle\langle N_B\rangle} \\ &= \left[\frac{1}{\langle N_A\rangle} + \frac{\omega_N - 1}{\langle N\rangle}\right] + \left[\frac{1}{\langle N_B\rangle} + \frac{\omega_N - 1}{\langle N\rangle}\right] - 2\frac{\omega_N - 1}{\langle N\rangle} \\ &= \frac{1}{\langle N_A\rangle} + \frac{1}{\langle N_B\rangle}. \end{aligned} \tag{17}$$

A comparison of the final result in Eq. (17) with Eq. (8) shows that the mixed-events procedure gives the same σ^2 for N_A/N_B fluctuations as in the GCE formulation for an ideal Boltzmann gas, i.e., for $\omega_A = \omega_B = 1$ and $\rho_{AB} = 0$. If $\omega_N = 1$ [e.g., for the Poisson distribution $P(N)$], one indeed finds $\omega_A^{\rm mix} = \omega_B^{\rm mix} = 1$ and $\rho_{AB}^{\rm mix} = 0$. Otherwise, if $\omega_N \neq 1$, the mixed-events procedure leads to $\omega_A^{\rm mix} \neq 1$, $\omega_B^{\rm mix} \neq 1$, and to nonzero $N_A N_B$ correlations, as seen from the second line of Eq. (17). Thus, if, e.g., event-by-event fluctuations in the total number of pions and kaons are stronger than Poissonian ones, i.e., $\omega_N > 1$, positive pion-kaon correlations appear in the mixed events. They lead to larger (smaller) N_K in the sample of mixed events with larger (smaller) N_π. However, the final result for $\sigma^2_{\rm mix}$ (17) is still the same as for $\omega_N = 1$, it does not depend on the specific form of $P(N)$. Nontrivial ($\omega_{A,B}^{\rm mix} \neq 1$) fluctuations of N_A and N_B as well as nonzero $\rho_{AB}^{\rm mix}$ correlations may exist in the mixed-events procedure, but they are canceled out in $\sigma^2_{\rm mix}$.

III. FLUCTUATIONS OF RATIOS IN STATISTICAL MODELS

A. Quantum statistics and resonance decays

The occupation numbers, $n_{\mathbf{p},j}$, of single quantum states (with fixed projection of particle spin) labeled by the momentum vector $\mathbf{p}$ are equal to $n_{\mathbf{p},j} = 0, 1, \ldots, \infty$ for bosons and $n_{\mathbf{p},j} = 0, 1$ for fermions. Their average values are

$$\langle n_{\mathbf{p},j}\rangle = \frac{1}{\exp[(\epsilon_{\mathbf{p}j} - \mu_j)/T] - \alpha_j}, \tag{18}$$

and their fluctuations read

$$\begin{aligned} \langle(\Delta n_{\mathbf{p},j})^2\rangle_{\rm gce} &\equiv \langle(n_{\mathbf{p},j} - \langle n_{\mathbf{p},j}\rangle)^2\rangle_{\rm gce} \\ &= \langle n_{\mathbf{p},j}\rangle(1 + \alpha_j\langle n_{\mathbf{p},j}\rangle) \equiv v^2_{\mathbf{p},j}, \end{aligned} \tag{19}$$

where T is the system temperature, m_j is the mass of a particle j, $\epsilon_{\mathbf{p}j} = \sqrt{\mathbf{p}^2 + m_j^2}$ is the single-particle energy. The value of α_j depends on quantum statistics, i.e., $+1$ for bosons and -1 for fermions, while $\alpha_j = 0$ gives the Boltzmann approximation. The chemical potential μ_j of a species j equals the following: $\mu_j = q_j\mu_Q + b_j\mu_B + s_j\mu_S$, where q_j, b_j, s_j are the particle electric charge, baryon number, and strangeness, respectively, while μ_Q, μ_B, μ_S are the corresponding chemical potentials that regulate the average values of these global conserved charges in the GCE.

In the equilibrium hadron-resonance gas model the mean number of primary particles (or resonances) is calculated as:

$$\langle N_j^*\rangle \equiv \sum_{\mathbf{p}}\langle n_{\mathbf{p},j}\rangle = \frac{g_j V}{2\pi^2}\int_0^\infty p^2 dp\, \langle n_{\mathbf{p},j}\rangle, \tag{20}$$

where V is the system volume and g_j is the degeneracy factor of a particle of species j (the number of spin states). In the thermodynamic limit, $V \to \infty$, the sum over the momentum states can be substituted by a momentum integral.

It is convenient to introduce a microscopic correlator, $\langle\Delta n_{\mathbf{p},j}\Delta n_{\mathbf{k},i}\rangle$, which in the GCE has the simple form:

$$\langle\Delta n_{\mathbf{p},j}\Delta n_{\mathbf{k},i}\rangle_{\rm gce} = v^2_{\mathbf{p},j}\,\delta_{ij}\,\delta_{\mathbf{pk}}. \tag{21}$$

Hence there are no correlations between different particle species, $i \neq j$, and/or between different momentum states, $\mathbf{p} \neq \mathbf{k}$. Only the Bose enhancement, $v^2_{\mathbf{p},j} > \langle n_{\mathbf{p},j}\rangle$ for $\alpha_j = 1$, and the Fermi suppression, $v^2_{\mathbf{p},j} < \langle n_{\mathbf{p},j}\rangle$ for $\alpha_j = -1$, exist for fluctuations of primary particles in the GCE. The correlator (1) can be presented in terms of microscopic correlators (21):

$$\langle \Delta N^*_j \Delta N^*_i \rangle_{\rm gce} = \sum_{\mathbf{p},\mathbf{k}} \langle \Delta n_{\mathbf{p},j} \Delta n_{\mathbf{k},i}\rangle_{\rm gce} = \delta_{ij} \sum_{\mathbf{p}} v^2_{\mathbf{p},j}. \quad (22)$$

In the case $i = j$ Eq. (22) gives the variance of primordial particles (before resonance decays) in the GCE.

For the hadron resonance gas formed in relativistic $A + A$ collisions the corrections due to quantum statistics (Bose enhancement and Fermi suppression) are small.[3] For the pion gas at $T = 160$ MeV, one finds $\omega_\pi \cong 1.1$ instead of $\omega = 1$ for Boltzmann particles. The quantum statistics effects are even smaller for heavier particles like kaons and almost negligible for resonances.

The average final (after resonance decays) multiplicities $\langle N_i\rangle$ are equal to:

$$\langle N_i\rangle \;=\; \langle N^*_i\rangle + \sum_R \langle N_R\rangle \langle n_i\rangle_R. \quad (23)$$

In Eq. (23), N^*_i denotes the number of stable primary hadrons of species i, the summation $\sum_R$ runs over all types of resonances R, and $\langle n_i\rangle_R \equiv \sum_r b^R_r n^R_{i,r}$ is the average over resonance decay channels. The parameters b^R_r are the branching ratios of the r-th branches; $n^R_{i,r}$ is the number of particles of species i produced in resonance R decays via a decay mode r. The index r runs over all decay channels of a resonance R with the requirement $\sum_r b^R_r = 1$. In the GCE the correlator (1) after resonance decays can be calculated as [35]:

$$\langle \Delta N_A \Delta N_B\rangle_{\rm gce} = \langle \Delta N^*_A \Delta N^*_B\rangle_{\rm gce} + \sum_R \Big[\big\langle \Delta N^2_R\big\rangle \langle n_A\rangle_R \langle n_B\rangle_R + \langle N_R\rangle \langle \Delta n_A \Delta n_B\rangle_R\Big], \quad (24)$$

where $\langle \Delta n_A \Delta n_B\rangle_R \equiv \sum_r b^R_r n^R_{A,r} n^R_{B,r} - \langle n_A\rangle_R \langle n_B\rangle_R$.

B. Global conservation laws

In the MCE, the energy and conserved charges are fixed exactly for each microscopic state of the system. This leads to two modifications in comparison with the GCE. First, additional terms appear for the primordial microscopic correlators in the MCE. They reflect the (anti-)correlations between different particles, $i \neq j$, and different momentum levels, $\mathbf{p} \neq \mathbf{k}$, due to charge and energy conservation in the MCE [14],

$$\begin{aligned}\langle \Delta n_{\mathbf{p},j} \Delta n_{\mathbf{k},i}\rangle_{\rm mce} &= v^2_{\mathbf{p},j}\,\delta_{ij}\,\delta_{\mathbf{pk}} \;-\; \frac{v^2_{\mathbf{p},j} v^2_{\mathbf{k},i}}{|A|}\,[\, q_i q_j M_{qq} + b_i b_j M_{bb} + s_i s_j M_{ss} \\ &+ (q_i s_j + q_j s_i) M_{qs} - (q_i b_j + q_j b_i) M_{qb} \\ &- (b_i s_j + b_j s_i) M_{bs} + \epsilon_{\mathbf{p}j}\epsilon_{\mathbf{k}i} M_{\epsilon\epsilon} - (q_i \epsilon_{\mathbf{p}j} + q_j \epsilon_{\mathbf{k}i}) M_{q\epsilon} \\ &+ (b_i \epsilon_{\mathbf{p}j} + b_j \epsilon_{\mathbf{k}i}) M_{b\epsilon} - (s_i \epsilon_{\mathbf{p}j} + s_j \epsilon_{\mathbf{k}i}) M_{s\epsilon}\,], \end{aligned} \quad (25)$$

where $|A|$ is the determinant and M_{ij} are the minors of the following matrix,

$$A = \begin{Bmatrix} \Delta(q^2) & \Delta(bq) & \Delta(sq) & \Delta(\epsilon q) \\ \Delta(qb) & \Delta(b^2) & \Delta(sb) & \Delta(\epsilon b) \\ \Delta(qs) & \Delta(bs) & \Delta(s^2) & \Delta(\epsilon s) \\ \Delta(q\epsilon) & \Delta(b\epsilon) & \Delta(s\epsilon) & \Delta(\epsilon^2), \end{Bmatrix} \quad (26)$$

with the elements $\Delta(q^2) \equiv \sum_{\mathbf{p},j} q^2_j v^2_{\mathbf{p},j}$, $\Delta(qb) \equiv \sum_{\mathbf{p},j} q_j b_j v^2_{\mathbf{p},j}$, $\Delta(q\epsilon) \equiv \sum_{\mathbf{p},j} q_j \epsilon_{\mathbf{p}j} v^2_{\mathbf{p},j}$, and so on. The sum, $\sum_{\mathbf{p},j}$, means integration over momentum $\mathbf{p}$ and the summation over all hadron-resonance species j contained in the model. The first term in the right-hand side of Eq. (25) corresponds to the microscopic correlator (21) in the GCE. Note, that the presence of the terms containing the single particle energy $\epsilon_{\mathbf{p}j} = \sqrt{\mathbf{p}^2 + m^2_j}$ in Eq. (25) is a consequence of energy conservation. In the CE, only charges are conserved, thus the terms containing $\epsilon_{\mathbf{p}j}$ in Eq. (25) are absent. The matrix A in Eq. (26) then becomes a 3×3 matrix (see Ref. [13]). An important property of the microscopic correlator method is that the particle number fluctuations and the correlations in the MCE or CE, although being different from those in the GCE, are expressed by quantities calculated within the GCE. The microscopic correlator (25) can be used to calculate the primordial particle (or resonances) correlator in the MCE (or in the CE):

$$\langle \Delta N_i \Delta N_j\rangle_{\rm mce} = \sum_{\mathbf{p},\mathbf{k}} \langle \Delta n_{\mathbf{p},i} \Delta n_{\mathbf{k},j}\rangle_{\rm mce}. \quad (27)$$

A second feature of the MCE (or CE) is the modification of the resonance decay contribution to the fluctuations in comparison to the GCE (24). In the MCE (or CE) it reads [13,14]:

$$\begin{aligned}\langle \Delta N_A\, \Delta N_B\rangle_{\rm mce} &= \langle \Delta N^*_A \Delta N^*_B\rangle_{\rm mce} + \sum_R \langle N_R\rangle\, \langle \Delta n_A\, \Delta n_B\rangle_R \\ &+ \sum_R \langle \Delta N^*_A \Delta N_R\rangle_{\rm mce} \langle n_B\rangle_R + \sum_R \langle \Delta N^*_B \Delta N_R\rangle_{\rm mce} \langle n_A\rangle_R \\ &+ \sum_{R,R'} \langle \Delta N_R \Delta N_{R'}\rangle_{\rm mce} \langle n_A\rangle_R \langle n_B\rangle_{R'}. \end{aligned} \quad (28)$$

Additional terms in Eq. (28) compared to Eq. (24) are due to the correlations (for primordial particles) induced by energy and charge conservations in the MCE. Equation (28) has the same form in the CE [13] and MCE [14]; the difference between these two ensembles appears because of different microscopic correlators (25). The microscopic correlators of the MCE together with Eq. (27) should be used to calculate the correlators $\langle \Delta N^*_A \Delta N^*_B\rangle_{\rm mce}$, $\langle \Delta N^*_A\, \Delta N_R\rangle_{\rm mce}$, $\langle \Delta N^*_A\, \Delta N_R\rangle_{\rm mce}$, $\langle \Delta N^*_B\, \Delta N_R\rangle_{\rm mce}$, and $\langle \Delta N_R\, \Delta N_{R'}\rangle_{\rm mce}$ entering in Eq. (28). The correlators (28) define finally the scaled variances ω_A and ω_B (2) and correlations ρ_{AB} (3) between the N_A and N_B numbers. Together with the average multiplicities $\langle N_A\rangle$ and $\langle N_B\rangle$ they define completely the fluctuations σ^2 (7) of the A to B number ratio.

[3] Possible strong Bose effects are discussed in Ref. [12].

IV. STATISTICAL AND HSD MODEL RESULTS FOR THE K/π RATIO

In this section we present the results of the hadron-resonance gas statistical model (SM) and the HSD transport model for the fluctuations of the K/π ratio in central nucleus-nucleus collisions. To carry out the SM calculations one has to fix the chemical freeze-out parameters. The dependence of the chemical potential μ_B on the collision energy is parameterized as [25]: $\mu_B(\sqrt{s_{NN}}) = 1.308\ \text{GeV} \times (1 + 0.273\sqrt{s_{NN}})^{-1}$, where the center-of-mass nucleon-nucleon collision energy, $\sqrt{s_{NN}}$, is taken in units of GeV. The system is assumed to be net strangeness free, i.e., $S = 0$, and to have the charge to baryon ratio of the initial colliding nuclei, i.e., $Q/B = 0.4$. These two conditions define the system strange, μ_S, and electric, μ_Q, chemical potentials. For the chemical freeze-out condition we chose the average energy per particle, $\langle E\rangle/\langle N\rangle = 1$ GeV [40]. Finally, the strangeness saturation factor, γ_S, is parameterized as in Ref. [26]: $\gamma_S = 1 - 0.396\exp(-1.23T/\mu_B)$. This determines all parameters of the model. An extended version of the THERMUS framework [41] is used for the SM calculations (for more details see Ref. [14]). Note that average multiplicities of pions and kaons measured in central nucleus-nucleus collisions at SPS and RHIC energies [42] are nicely described in the SM (see, e.g., Refs. [25,26]) as well as HSD (cf. Ref. [29]).

A. Results for ω_K, ω_π, and $\rho_{K\pi}$

According to Eq. (7) the fluctuations of the $K = K^+ + K^-$ to $\pi = \pi^+ + \pi^-$ ratio is given by

$$\sigma^2 = \frac{\omega_K}{\langle N_K\rangle} + \frac{\omega_\pi}{\langle N_\pi\rangle} - 2\rho_{K\pi}\left[\frac{\omega_K\omega_\pi}{\langle N_K\rangle\langle N_\pi\rangle}\right]^{1/2}. \quad (29)$$

The values of ω_π, ω_K, and $\rho_{K\pi}$ in different statistical ensembles are presented in Table I and for the HSD simulations of Pb + Pb (Au + Au) central (with impact parameter $b = 0$) collisions in Table II. Both the SM and HSD results are shown in Figs. 1 and 2. Let us first comment the SM results. In the SM the scaled variances ω_π and ω_K and correlation parameter

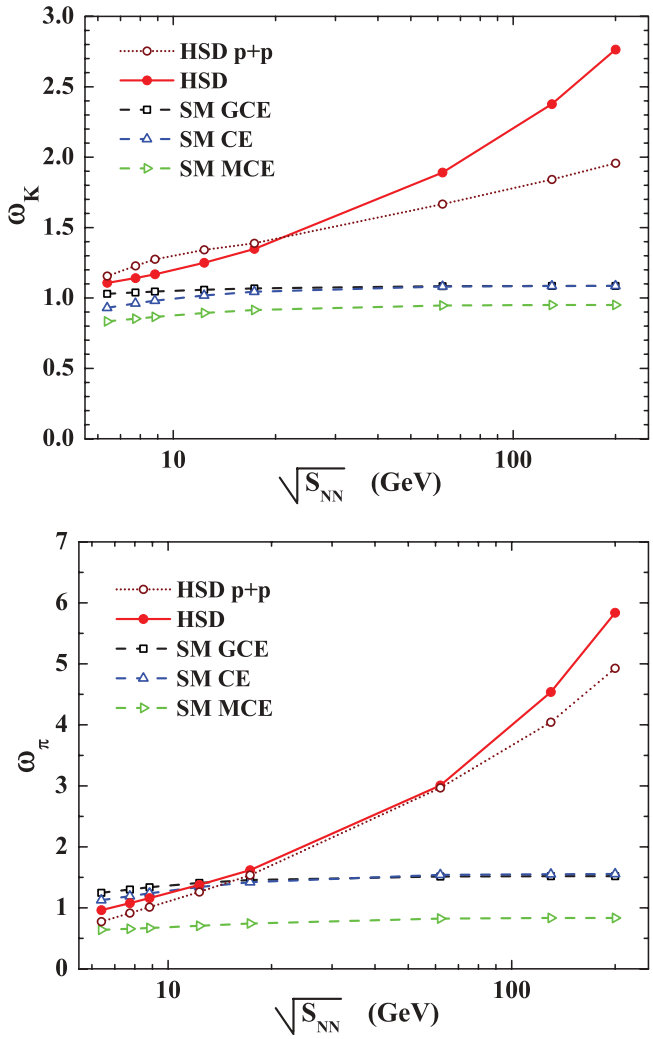

FIG. 1. (Color online) The SM results in the GCE, CE, and MCE ensembles and the HSD results (impact parameter $b = 0$) are presented for the scaled variances ω_π, ω_K for Pb + Pb (Au + Au) collisions at different center-of-mass energies $\sqrt{s_{NN}}$. For comparison the HSD results for inelastic proton-proton collisions are also presented in terms of the dotted lines with open circles.

TABLE I. The chemical freeze-out parameters T and μ_B for central Pb + Pb (Au + Au) collisions at different center-of-mass energies $\sqrt{s_{NN}}$. The hadron-resonance gas model results are presented for final (after resonance decays) number densities of pions n_π and kaons n_K (they are the same in all statistical ensembles), scaled variances ω_π, ω_K and correlation parameter $\rho_{K\pi}$ in the GCE, CE, and MCE.

$\sqrt{s_{NN}}$ (GeV)	T (MeV)	μ_B (MeV)	n_π (fm^{-3})	n_K (fm^{-3})	GCE			CE			MCE		
					ω_π	ω_K	$\rho_{K\pi}$	ω_π	ω_K	$\rho_{K\pi}$	ω_π	ω_K	$\rho_{K\pi}$
6.27	130.7	482.4	0.106	0.011	1.247	1.030	0.055	1.122	0.930	0.038	0.641	0.833	−0.243
7.62	138.3	424.6	0.134	0.016	1.301	1.039	0.066	1.184	0.961	0.049	0.656	0.853	−0.249
8.77	142.9	385.4	0.155	0.020	1.337	1.045	0.073	1.228	0.980	0.057	0.669	0.866	−0.251
12.3	151.5	300.1	0.202	0.029	1.408	1.058	0.086	1.324	1.018	0.074	0.705	0.893	−0.242
17.3	157	228.6	0.239	0.038	1.457	1.068	0.095	1.397	1.044	0.087	0.743	0.915	−0.226
62.4	163.1	72.7	0.293	0.055	1.514	1.084	0.110	1.506	1.081	0.109	0.824	0.947	−0.186
130	163.6	36.1	0.298	0.058	1.519	1.086	0.112	1.516	1.085	0.111	0.833	0.950	−0.181
200	163.7	23.4	0.298	0.058	1.519	1.086	0.112	1.519	1.085	0.112	0.835	0.950	−0.180

TABLE II. The HSD average multiplicities $\langle N_\pi \rangle$, $\langle N_K \rangle$ and values of ω_π, ω_K, and $\rho_{K\pi}$ for central (impact parameter $b = 0$) Pb + Pb (Au + Au) collisions at different center-of-mass energies $\sqrt{s_{NN}}$.

$\sqrt{s_{NN}}$ (GeV)	HSD full acceptance				
	$\langle N_\pi \rangle$	$\langle N_K \rangle$	ω_π	ω_K	$\rho_{K\pi}$
6.27	612.03	43.329	0.961	1.107	−0.091
7.62	732.11	60.801	1.077	1.141	−0.063
8.77	823.71	75.133	1.159	1.168	−0.033
12.3	1072.3	116.44	1.378	1.250	0.046
17.3	1364.6	165.52	1.619	1.348	0.126
62.4	2933.9	449.29	3.006	1.891	0.412
130	4304.2	692.59	4.538	2.378	0.557
200	5204.0	861.77	5.838	2.765	0.634

$\rho_{K\pi}$ approach finite values in the thermodynamic limit of large volumes. These limiting values are presented in Table I and in Figs. 1 and 2. For central Pb + Pb and Au + Au collisions the corresponding volumes in the SM are large enough. Finite volume corrections are expected to be on the level of a few percentages. The finite volume effects for the scaled variances and correlation parameters in the CE and MCE are, however, difficult to calculate (see Ref. [15]) and they will not be considered in the present article. The GCE values of ω_π and ω_K reflect the Bose statistics of pions and kaons and the contributions from resonance decays.

The π-K correlations $\rho_{K\pi}$ are due to resonances having simultaneously K and π mesons in their decay products. In the hadron-resonance gas within the GCE ensemble, these quantum statistics and resonance decay effects are responsible for deviations of ω_K and ω_π from 1, and of $\rho_{K\pi}$ from 0. The most important effect of an exact charge conservation in the CE ensemble is a suppression of the kaon number fluctuation. This happens mainly due to exact strangeness conservation and is reflected in smaller CE values of ω_K at low collision energies in comparison to those from the GCE ensemble. The MCE values of ω_K and ω_π are further suppressed in comparison those from the CE ensemble, which is due to exact energy conservation. The effect is stronger for pions than for kaons since pions carry a larger part of the total energy. An important feature of the MCE is the anticorrelation between N_π and N_K, i.e., negative values of $\rho_{K\pi}$. This is also a consequence of energy conservation for each microscopic state of the system in the MCE [14]. The presented results demonstrate that global conservation laws are rather important for the values of ω_π, ω_K, and $\rho_{K\pi}$. In particular, the exact energy conservation strongly suppresses the fluctuations in the pion and kaon numbers and leads to $\omega_K < 1$ and $\omega_\pi < 1$ in the MCE ensemble instead of $\omega_K > 1$ and $\omega_\pi > 1$ in the GCE and CE ensembles. The exact energy conservation changes also the π-K correlation into an anticorrelation: instead of $\rho_{K\pi} > 0$ in the GCE and CE ensembles one finds $\rho_{K\pi} < 0$ in the MCE.

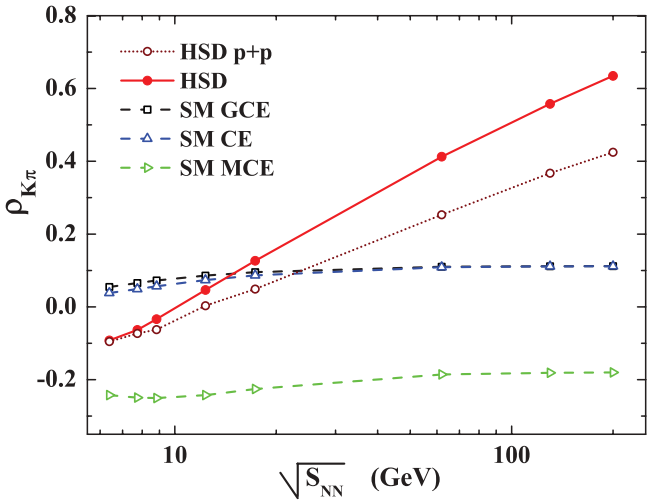

FIG. 2. (Color online) The SM results in the GCE, CE, and MCE ensembles and the HSD results (impact parameter $b = 0$) are presented for the correlation parameter $\rho_{K\pi}$ for Pb + Pb (Au + Au) collisions at different center-of-mass energies $\sqrt{s_{NN}}$. For comparison the HSD results for inelastic proton-proton collisions are also presented by the dotted line with open circles.

As seen from Figs. 1 and 2 the HSD results for ω_π, ω_K, and $\rho_{K\pi}$ (solid lines) are rather different from those in the SM. For a comparison the HSD results for inelastic proton-proton collisions are also presented in Figs. 1 and 2 (dotted lines). The HSD scaled variances ω_π and ω_K increase at higher energies. A similar behavior has been observed earlier in Ref. [21] for the scaled variance of all charged hadrons. The HSD calculations reveal the anticorrelation between N_π and N_K, i.e., negative values of $\rho_{K\pi}$, for low SPS energies, where the influence of conservation laws is more stringent.

Comparing this result with the SM (in different ensembles) one may conclude that negative values of $\rho_{K\pi}$ in HSD appear because of a dominant role of energy conservation in joint π-K production at small collision energies. The HSD values of $\rho_{K\pi}$ become, however, positive and strongly increases with increasing collision energy. This is due to the contribution of heavy strings to joint π-K (or K^*) production at high energies in the HSD simulations. Note that the HSD results for ω_π, ω_K, and $\rho_{K\pi}$ in nucleus-nucleus collisions become larger than those in proton-proton inelastic reactions at high collision energies. This is due to an increase of secondary (i.e., meson-baryon and meson-meson) collisions at higher bombarding energy. Thus, a strong deviation of HSD from the SM with increasing energies is a consequence of nonequilibrium dynamics in the hadron-string model that is driven by the formation of heavy strings and their decay. Indeed, future experimental data on the fluctuations of K, π and $K\pi$ correlations will allow us to shed more light on the equilibration pattern achieved in heavy-ion collisions at RHIC energies.

Two comments are appropriate here. The first one concerns a correspondence between the HSD and SM results. In HSD three charges—net baryon number B (equal to the number of participating nucleons), net electric charge Q (equal to the number of participating protons), and net strangeness S (equal to zero)—are conserved exactly during the system evolution. However, B and Q can fluctuate from event to event because of the fluctuations in the number of nucleon participants. They also cause fluctuations of the energy of produced hadrons in

the HSD simulations. Moreover, an essential part of the system energy is transformed to collective motion. Thus, even in the sample of the HSD events with fixed number of participants, the thermal energy of the created particles can fluctuate from event to event. Both the charge and energy fluctuations in HSD are not of thermal origin. Therefore, an attempt to interpret the HSD multiplicity fluctuations in statistical terms would require use of a more general concept of statistical ensembles with fluctuating extensive quantities [17,18]. In particular, large values of the scaled variances, $\omega_i \sim \langle N_i \rangle$, in high-energy proton-proton collisions are also present in the HSD simulations of nucleus-nucleus collisions. In the SM model this would require a special form of scaling volume fluctuations as recently suggested in Ref. [19].

Our second comment concerns the physical origin of the correlation parameter $\rho_{K\pi}$. Two sources of the π-K correlations are resonance, string decays, and electric charge conservation. To estimate their relative weights, one can benefit from measuring the correlations $\rho_{K\pi}$ in the separate charge channels: $\pi^- K^-$ and $\pi^- K^+$ as suggested in Ref. [43]. The resonances decaying into $\pi^- K^+$ produce the corresponding correlation, while an analogous correlation in the $\pi^- K^-$ system is absent. Note that electric charge conservation leads also to qualitatively different correlation effects in $\pi^- K^-$ and $\pi^- K^+$ channels.

B. Results for σ, $\sigma_{\rm mix}$, and $\sigma_{\rm dyn}$

The fluctuation in the kaon-to-pion ratio is dominated by the fluctuations of kaons alone because the average multiplicity of kaons is about 10 times smaller than that of pions. Thus, the first term in the right-hand side of Eq. (29) gives the dominant contribution, whereas the second and third terms in Eq. (29) give only small corrections. The model calculations of Eq. (29) require, in addition to ω_K, ω_π, and $\rho_{K\pi}$ values, the knowledge of the average multiplicities $\langle N_K \rangle$ and $\langle N_\pi \rangle$. For the HSD simulations (impact parameter $b = 0$ in Pb + Pb collisions at SPS energies and Au + Au collisions at RHIC) the corresponding average multiplicities are presented in Table II. To fix average multiplicities in the SM one needs to choose the system volume. For each collision energy we fix the volume of the statistical system to obtain the same kaon average multiplicity in the SM as in the HSD calculations: $\langle N_K \rangle_{\rm stat} = \langle N_K \rangle_{\rm HSD}$. We recall that average multiplicities of kaons and pions are the same in all statistical ensembles. The SM volume in central Pb + Pb (Au + Au) collisions is large enough and all statistical ensembles are thermodynamically equivalent for the average pion and kaon multiplicities since these multiplicities are much larger than 1.

In Fig. 3 the values of σ (in percentages)—calculated according to Eq. (29) and Eq. (17)—are presented in the left and right panels, respectively, for the SM in different ensembles as well as for the HSD simulations. The first conclusion from Fig. 3 (left) is that all results for σ in the different models are rather similar. One observes a monotonic decrease of σ with collision energy. This is just because of an increase of the kaon and pion average multiplicities with collision energy. The mixed-event fluctuations $\sigma_{\rm mix}$ in the

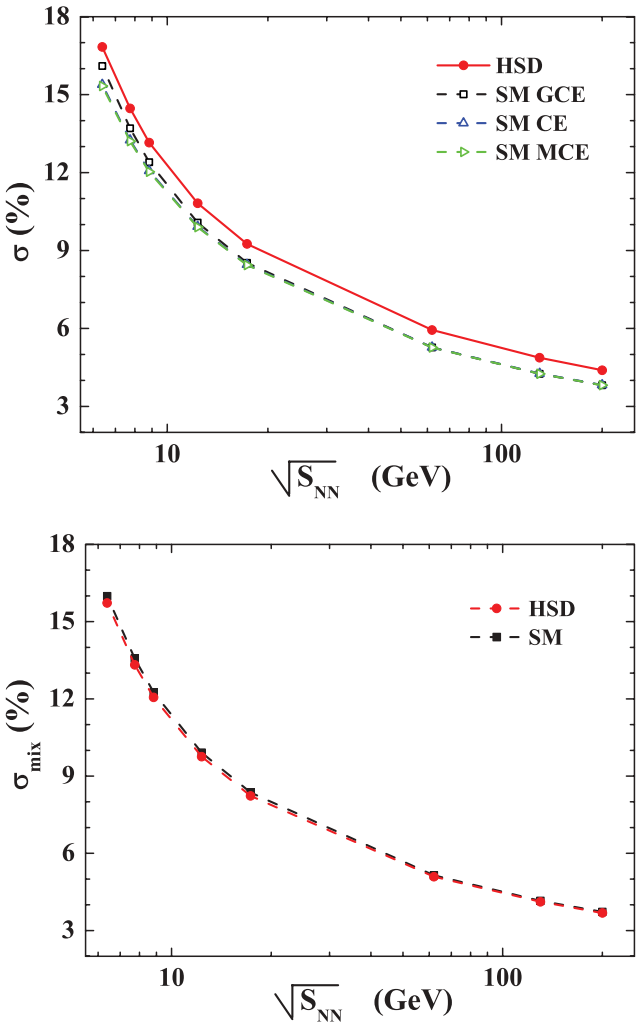

FIG. 3. (Color online) (Left) The SM results in the GCE, CE, and MCE ensembles as well as the HSD results (impact parameter $b = 0$) are presented for $\sigma \times 100\%$ defined by Eq. (29) for Pb + Pb (Au + Au) collisions at different center-of-mass energies $\sqrt{s_{NN}}$. (Right) The same as in the left panel but for $\sigma_{\rm mix} \times 100\%$ in mixed events defined by Eq. (17), $\sigma^2_{\rm mix} = 1/\langle N_K \rangle + 1/\langle N_\pi \rangle$.

model analysis are fully defined by these average multiplicities according to Eq. (17). The values of $\sigma_{\rm mix}$ are therefore the same in the different statistical ensembles. They are also very close to the HSD values because we have fixed the statistical system volume to obtain the same kaon average multiplicities in the statistical model as in HSD at each collision energy. As seen from Fig. 3 (right) the requirement of $\langle N_K \rangle_{\rm stat} = \langle N_K \rangle_{\rm HSD}$ leads to practically equal values of $\sigma_{\rm mix}$ in both HSD and the SM.

Differences between the statistical ensembles as well as between the statistical and HSD results become visible for other measures of K/π fluctuations such as $\sigma_{\rm dyn}$ defined by Eq. (9) and $F = \sigma^2/\sigma^2_{\rm mix}$. They are shown in Fig. 4, (left) and (right), respectively. At small collision energies the CE and MCE results in Fig. 4 demonstrate negative values of $\sigma_{\rm dyn}$, respectively $F < 1$. When the collision energy increases, $\sigma_{\rm dyn}$ in the CE and MCE ensembles becomes positive, i.e., $F > 1$. Moreover, the different statistical ensembles approach

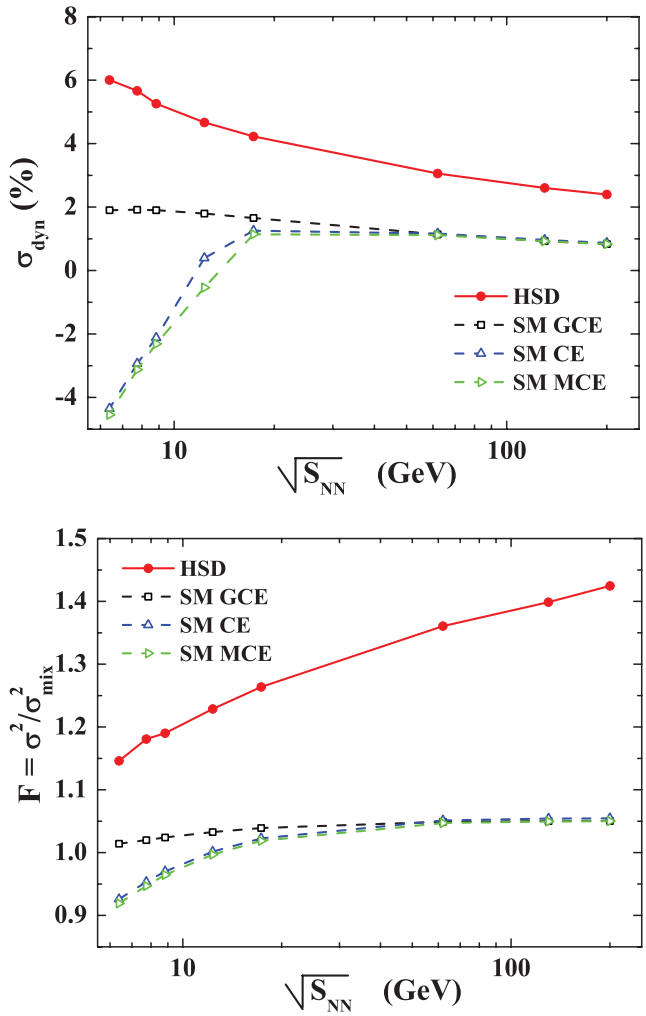

FIG. 4. (Color online) (Left) The results for the K/π fluctuations at different center-of-mass energies $\sqrt{s_{NN}}$ in the GCE, CE, and MCE ensembles as well as from HSD (impact parameter $b = 0$) are presented for $\sigma_{\rm dyn} \times 100\%$ defined by Eq. (9). (Right) The same as in the left panel but for $F = \sigma^2/\sigma^2_{\rm mix}$.

the same values of $\sigma_{\rm dyn}$ and F at high collision energy. In the SM the values of σ and $\sigma_{\rm mix}$ approach zero at high collision energies due to an increase of the average multiplicities. The same limit should be also valid for $\sigma_{\rm dyn}$ in the SM. In contrast, the measure F shows a different behavior at high energies: the SM gives $F \cong 1.05$ in the high energy limit, while the HSD result for F demonstrates a monotonic increase with collision energy. An interesting feature of the SM is approximately the same result for σ (and, thus, $\sigma_{\rm dyn}$ and F) in the CE and MCE ensembles. From Table I and Figs. 1 and 2 one observes that ω_K, ω_π, and $\rho_{K\pi}$ are rather different in the CE and MCE. Thus, as discussed above, an exact energy conservation influences the particle scaled variances and correlations. These changes are, however, canceled out in the fluctuations of the kaon-to-pion ratio.

C. Volume fluctuations

It has been mentioned in the literature (see, e.g., Ref. [34]) that the particle number ratio is independent of volume fluctuations because both multiplicities are proportional to the volume. In fact, the *average multiplicities* $\langle N_K \rangle$ and $\langle N_\pi \rangle$, but not N_K and N_π, are proportional to the system volume. Let us consider the problem in the SM assuming the presence of volume fluctuations at fixed values of T and μ_B. This assumption corresponds approximately to volume fluctuations in nucleus-nucleus collisions from different impact parameters in each collision event. Under these assumptions the SM values in Table I remain the same for any volume (if only this volume is large enough and the finite size corrections can be neglected). However, the average hadron multiplicities are proportional to the volume. Therefore, the SM result for σ^2 reads, $\sigma^2 = \sigma_0^2 V_0/V$, where V_0 is the average system volume and σ_0^2 is calculated for the average multiplicities corresponding to this average volume V_0. Expanding $V_0/V = V_0/(V_0 + \delta V)$ in powers of $\delta V/V_0$, one finds to second order in $\delta V/V_0$,

$$\sigma^2 \cong \sigma_0^2 \left[1 + \frac{\langle (\delta V)^2 \rangle}{V_0^2}\right], \tag{30}$$

where

$$\langle (\delta V)^2 \rangle = \int dV (V - V_0)^2 \, W(V) \tag{31}$$

corresponds to an average over the volume distribution function $W(V)$ that describes the volume fluctuations. As clearly seen from Eq. (30) the volume fluctuations influence, of course, the K/π particle number fluctuations and make them larger. Comparing the K/π particle number fluctuations in, e.g., 1% of most central nucleus-nucleus collisions with those in, e.g., 10% one should take into account two effects. First, in the 10% sample the average volume V_0 is smaller than that in 1% sample and, thus, σ_0^2 in Eq. (30) is larger. Second, the volume fluctuations (31) in the 10% sample is larger, and this gives an additional contribution to σ^2 according to Eq. (30).

One may also consider volume fluctuations at fixed energy and conserved charges (see, e.g., Ref. [19]). In this case the connection between the average multiplicity and the volume becomes more complicated. The volume fluctuation within the MCE ensemble can strongly affect the fluctuations in the particle number ratios. This possibility will be discussed in more detail in a forthcoming study.

V. EXCITATION FUNCTION FOR THE K/π RATIO: COMPARISON WITH DATA

A comparison of the SM results for K/π fluctuations in different ensembles with the data looks problematic at present. This is because of difficulties with implementing the experimental acceptance in the SM (see a discussion of this point in Ref. [16]). A similar problem exists in the SM with chemical nonequilibrium effects discussed in Ref. [44]. The experimental acceptance can be taken into account in the transport code. To compare the HSD calculations with the measured data the experimental cuts are applied for the simulated set of the HSD events. In Fig. 5 the HSD results for the excitation function in $\sigma_{\rm dyn}$ (9) for the K/π ratio is shown in comparison with the experimental data measured by

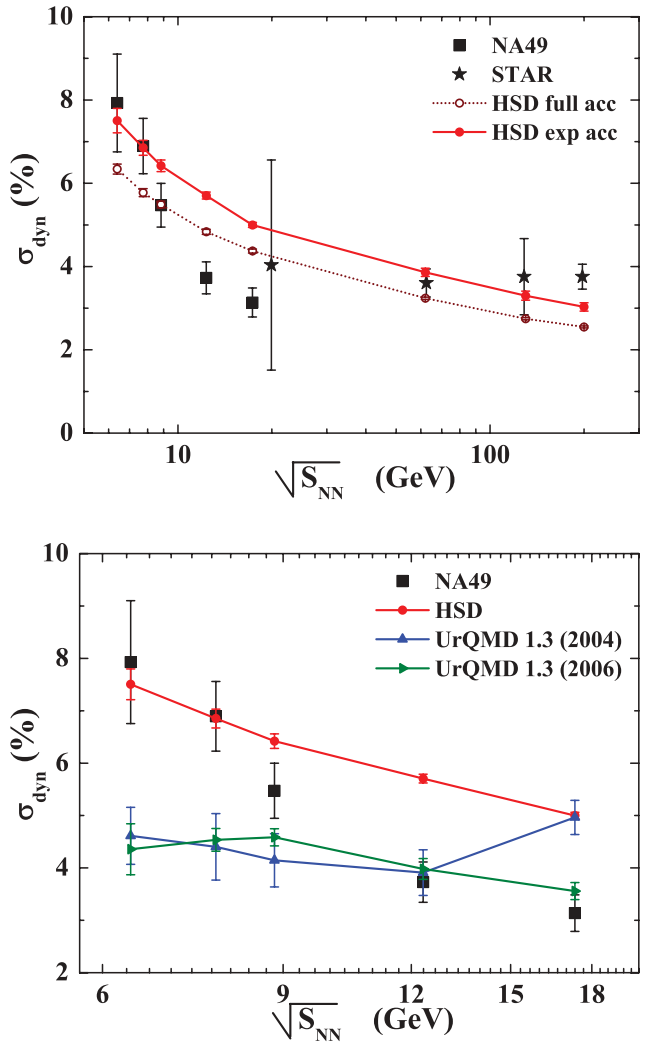

FIG. 5. (Color online) (Left) The HSD results for the excitation function in $\sigma_{\rm dyn}$ (9) for the K/π ratio for full acceptance (dotted line) and within the experimental acceptance (solid line) in comparison to the experimental data measured by the NA49 Collaboration at the CERN SPS [7] and by the STAR Collaboration at BNL RHIC [8]. 3.5% most central HSD events were selected for the analysis for SPS energies and 5% for the RHIC energies. (Right) The HSD results (circles) and two different versions of UrQMD (triangles) calculations [36,45] for $\sigma_{\rm dyn}$ versus the NA49 data. Statistical uncertainties in the transport calculations are shown by error bars.

the NA49 Collaboration at the CERN SPS [7] and by the STAR Collaboration at BNL RHIC [8].

For the SPS energies we used a cut $p_{\rm lab} \geqslant 3$ GeV/c applied by NA49 to provide a precise particle identification. For the RHIC energies the cuts are in pseudorapidity, $|\eta| < 1$, and in the transverse momentum, $0.2 < p_T < 0.6$ GeV/c, Ref. [8]. We note also that the HSD results presented in Fig. 5 correspond to the specific centrality selections as in the experiment—the NA49 data correspond to the 3.5% most central collisions selected via the veto calorimeter, whereas in the STAR experiment the 5% most central events with the highest multiplicities in the pseudorapidity range $|\eta| < 0.5$ have been selected.

The HSD results—within the acceptance cuts—are shown in Fig. 5 (left) as solid lines. In addition in the left-hand side of Fig. 5 the result for the full acceptance is indicated by a dotted line. One can see that the experimental cuts lead to a systematic increase of $\sigma_{\rm dyn}$; however, they do not change the shape of the excitation function. By comparing the full acceptance line to those in Fig. 4 (left) for $b = 0$ one sees also a small enhancement of $\sigma_{\rm dyn}$ that is due to slight decrease of the hadron multiplicities and, correspondingly, increase of those fluctuations.

In the right panel of Fig. 5 the HSD results for $\sigma_{\rm dyn}$ within the experimental acceptance are compared with two different versions of UrQMD v1.3 simulations [36,45] and the NA49 data in the SPS energy range. The remaining differences between the UrQMD v1.3 calculations from 2006 and 2004 at 160 A GeV can be attributed to the differences in implementation of acceptance cuts (cf. discussion in Ref. [45]). One sees that the UrQMD model gives practically a constant $\sigma_{\rm dyn}$, which is about 40% smaller than the results from HSD at the lowest SPS energy. This difference between the two transport models might be attributed to different realizations of the string and resonance dynamics in HSD and UrQMD: in UrQMD the strings decay first to heavy baryonic and mesonic resonances that only later decay to "light" hadrons such as kaons and pions. In HSD the strings dominantly decay directly to "light" hadrons (from the pseudoscalar meson octet) or the vector mesons ρ, ω, and K^* (or the baryon octet and decouplet in case of baryon number ± 1). As discussed in the previous section, $\sigma_{\rm dyn}$ is indeed very sensitive to the model details at low bombarding energies: the SM in different ensembles and the HSD give rather different behavior at the low SPS energies [cf. Fig. 4 (left)].

Although the UrQMD results are available presently only up to the top SPS energy, the HSD model shows a good agreement with the recent STAR data [8] [cf. Fig. 5 (left)]. A good agreement with the STAR data [46] for K/π ratio fluctuations in Cu+Cu at $\sqrt{s_{NN}} = 200$ GeV was also obtained in the multiphase transport model (AMPT) [47]. This is in contrast to the corresponding result from the Heavy Ion Jet Interaction Generator (HIJING) model [48] that overpredicts substantially the experimental data [46]. The difference has been attributed in Ref. [46] to an absence of the final rescattering in HIJING that is incorporated in AMPT as well as in HSD.

VI. SUMMARY AND CONCLUSIONS

We have studied the event-by-event fluctuations of the kaon to pion number ratio in central Au + Au (or Pb + Pb) collisions from low SPS up to top RHIC energies within the statistical hadron-resonance gas model for different statistical ensembles—GCE, CE, and MCE—and in the HSD transport approach. We have obtained substantial differences in the HSD and statistical model results for the scaled variances ω_K, ω_π and the correlation parameter $\rho_{K\pi}$ as presented in Figs. 1 and 2. Thus, the second moments of the multiplicity distributions may serve as a good probe for the amount of equilibration achieved in central nucleus-nucleus collisions. Note that the differences between the transport and statistical model results for

multiplicity fluctuations and correlations increase with collision energy (see Refs. [21,22]). There are also arguments that the behavior of higher moments of event-by-event multiplicities may serve as an important signature of the QCD critical point [49].

The observable $\sigma_{\rm dyn}$, which characterizes the fluctuations of the kaon to pion ratio, shows to be rather sensitive to the details of the model at low collision energies. The CE and MCE results in Fig. 4 demonstrate negative values for $\sigma_{\rm dyn}$, whereas the GCE gives approximately a constant positive value for $\sigma_{\rm dyn}$. The HSD results correspond to larger values of $\sigma_{\rm dyn}$ than those in the GCE statistical model. They even show an increase at lower SPS energies. When the collision energy increases, the quantity $\sigma_{\rm dyn}$ in the CE and MCE becomes positive. Moreover, the different statistical ensembles approach to the same values of $\sigma_{\rm dyn}$ at high collision energy. This is just because the values of σ and $\sigma_{\rm mix}$ approach zero at high collision energies. Thus, the same limit equal to zero should be also valid for $\sigma_{\rm dyn}$ in the statistical models. However, the measure $F = \sigma^2/\sigma^2_{\rm mix}$ shows another behavior at high energies. The statistical models give a constant value $F \cong 1.05$ in the high energy limit, whereas the HSD results for F demonstrate a monotonic increase with collision energy.

We find that the HSD model can qualitatively reproduce the measured excitation function for the K/π ratio fluctuations in central Au + Au (or Pb + Pb) collisions from low SPS up to top RHIC energies. We have shown that accounting for the experimental acceptance as well as the centrality selection has a relatively small influence on $\sigma_{\rm dyn}$ and does not change the shape of the $\sigma_{\rm dyn}$ excitation function. We conclude that the HSD hadron-string model—which does not have a QGP phase transition and not explicitly includes the quark and gluon degrees of freedom—can reproduce qualitatively the experimental excitation function. In particular, it gives the rise of $\sigma_{\rm dyn}$ with decreasing bombarding energy. This fact brings us to the conclusion that the observable enhancement of $\sigma_{\rm dyn}$ at low SPS energies might dominantly signal nonequilibrium string dynamics rather than a phase transition of hadronic to partonic matter or the QCD critical point.

ACKNOWLEDGMENTS

We thank M. Bleicher, W. Cassing, M. Gaździcki, W. Greiner, C. Höhne, D. Kresan, M. Mitrovski, T. Schuster, R. Stock, H. Ströbele, G. Torrieri, S. Wheaton, and O. S. Zozulya for useful discussions. This work was in part supported by the Program of Fundamental Researches of the Department of Physics and Astronomy of National Academy of Sciences, Ukraine.

[1] H. Heiselberg, Phys. Rep. **351**, 161 (2001); S. Jeon and V. Koch, in *Quark-Gluon Plasma 3*, edited by R. C. Hwa and X.-N. Wang (World Scientific, Singapore, 2004), pp. 430–490; T. K. Nayak, Int. J. Mod. Phys. E **16**, 3303 (2008); V. Koch, arXiv:0810.2520 [nucl-th].

[2] M. Gaździcki and M. I. Gorenstein, Acta Phys. Pol. B **30**, 2705 (1999); M. Gaździcki, M. I. Gorenstein, and St. Mrówczyński, Phys. Lett. **B585**, 115 (2004); M. I. Gorenstein, M. Gaździcki, and O. S. Zozulya, *ibid.* **B585**, 237 (2004).

[3] I. N. Mishustin, Phys. Rev. Lett. **82**, 4779 (1999); Nucl. Phys. **A681**, 56c (2001); H. Heiselberg and A. D. Jackson, Phys. Rev. C **63**, 064904 (2001).

[4] M. Stephanov, K. Rajagopal, and E. Shuryak, Phys. Rev. Lett. **81**, 4816 (1998); Phys. Rev. D **60**, 114028 (1999); M. Stephanov, Acta Phys. Pol. B **35**, 2939 (2004).

[5] S. V. Afanasev *et al.* (NA49 Collaboration), Phys. Rev. Lett. **86**, 1965 (2001).

[6] M. M. Aggarwal *et al.* (WA98 Collaboration), Phys. Rev. C **65**, 054912 (2002); J. Adams *et al.* (STAR Collaboration), *ibid.* **68**, 044905 (2003); C. Roland *et al.* (NA49 Collaboration), J. Phys. G **30**, S1381 (2004); Z. W. Chai *et al.* (PHOBOS Collaboration), J. Phys. Conf. Ser. **27**, 128 (2005); M. Rybczynski *et al.* (NA49 Collaboration), *ibid.* **5**, 74 (2005); J. T. Mitchell (PHENIX Collaboration), *ibid.* **27**, 88 (2005); C. Alt *et al.* (NA49 Collaboration), Phys. Rev. C **75**, 064904 (2007); C. Alt *et al.* (NA49 Collaboration), *ibid.* **78**, 034914 (2008); A. Adare *et al.* (PHENIX Collaboration), *ibid.* **78**, 044902 (2008).

[7] C. Alt *et al.* (NA49 Collaboration), arXiv:0808.1237 [nucl-ex].

[8] S. Das *et al.* (STAR Collaboration), J. Phys. G **32**, S541 (2006); B. I. Abelev *et al.*, arXiv:0901.1795 [nucl-ex].

[9] H. Appelshauser *et al.* (NA49 Collaboration), Phys. Lett. **B459**, 679 (1999); D. Adamova *et al.* (CERES Collaboration), Nucl. Phys. **A727**, 97 (2003); T. Anticic *et al.* (NA49 Collaboration), Phys. Rev. C **70**, 034902 (2004); S. S. Adler *et al.* (PHENIX Collaboration), Phys. Rev. Lett. **93**, 092301 (2004); J. Adams *et al.* (STAR Collaboration), Phys. Rev. C **71**, 064906 (2005).

[10] V. V. Begun, M. Gaździcki, M. I. Gorenstein, and O. S. Zozulya, Phys. Rev. C **70**, 034901 (2004).

[11] V. V. Begun, M. I. Gorenstein, and O. S. Zozulya, Phys. Rev. C **72**, 014902 (2005); A. Keränen, F. Becattini, V. V. Begun, M. I. Gorenstein, and O. S. Zozulya, J. Phys. G **31**, S1095 (2005); F. Becattini, A. Keränen, L. Ferroni, and T. Gabbriellini, Phys. Rev. C **72**, 064904 (2005); V. V. Begun, M. I. Gorenstein, A. P. Kostyuk, and O. S. Zozulya, *ibid.* **71**, 054904 (2005); J. Cleymans, K. Redlich, and L. Turko, *ibid.* **71**, 047902 (2005); J. Phys. G **31**, 1421 (2005); V. V. Begun, M. I. Gorenstein, A. P. Kostyuk, and O. S. Zozulya, J. Phys. G **32**, 935 (2006); M. I. Gorenstein, M. Hauer, and D. O. Nikolajenko, Phys. Rev. C **76**, 024901 (2007).

[12] V. V. Begun and M. I. Gorenstein, Phys. Rev. C **73**, 054904 (2006); Phys. Lett. **B653**, 190 (2007); Phys. Rev. C **77**, 064903 (2008).

[13] V. V. Begun, M. I. Gorenstein, M. Hauer, V. P. Konchakovski, and O. S. Zozulya, Phys. Rev. C **74**, 044903 (2006).

[14] V. V. Begun, M. Gaździcki, M. I. Gorenstein, M. Hauer, V. P. Konchakovski, and B. Lungwitz, Phys. Rev. C **76**, 024902 (2007).

[15] M. Hauer, V. V. Begun, and M. I. Gorenstein, Eur. Phys. J. C **58**, 83 (2008).

[16] M. Hauer, Phys. Rev. C **77**, 034909 (2008).

[17] M. I. Gorenstein and M. Hauer, Phys. Rev. C **78**, 041902(R) (2008).

[18] M. I. Gorenstein, J. Phys. G **35**, 125102 (2008).

[19] V. V. Begun, M. Gaździcki, and M. I. Gorenstein, Phys. Rev. C **78**, 024904 (2008); arXiv:0812.3078 [hep-ph].
[20] V. P. Konchakovski, S. Haussler, M. I. Gorenstein, E. L. Bratkovskaya, M. Bleicher, and H. Stöcker, Phys. Rev. C **73**, 034902 (2006); V. P. Konchakovski, M. I. Gorenstein, E. L. Bratkovskaya, and H. Stocker, Phys. Rev. C **74**, 064911 (2006); V. P. Konchakovski, M. I. Gorenstein, and E. L. Bratkovskaya, *ibid.* **76**, 031901(R) (2007).
[21] V. P. Konchakovski, M. I. Gorenstein, and E. L. Bratkovskaya, Phys. Lett. **B651**, 114 (2007).
[22] B. Lungwitz and M. Bleicher, Phys. Rev. C **76**, 044904 (2007).
[23] V. P. Konchakovski, B. Lungwitz, M. I. Gorenstein, and E. L. Bratkovskaya, Phys. Rev. C **78**, 024906 (2008).
[24] J. Cleymans and H. Satz, Z. Phys. C **57**, 135 (1993); J. Sollfrank, M. Gaździcki, U. Heinz, and J. Rafelski, *ibid.* **61**, 659 (1994); G. D. Yen, M. I. Gorenstein, W. Greiner, and S. N. Yang, *ibid.* **56**, 2210 (1997); F. Becattini, M. Gaździcki, and J. Solfrank, Eur. Phys. J. C **5**, 143 (1998); G. D. Yen and M. I. Gorenstein, Phys. Rev. C **59**, 2788 (1999); P. Braun-Munzinger, I. Heppe, and J. Stachel, Phys. Lett. **B465**, 15 (1999); P. Braun-Munzinger, D. Magestro, K. Redlich, and J. Stachel, *ibid.* **B518**, 41 (2001); F. Becattini, M. Gaździcki, A. Keränen, J. Manninen, and R. Stock, Phys. Rev. C **69**, 024905 (2004); A. Andronic, P. Braun-Munzinger, and J. Stachel, Nucl. Phys. **A772**, 167 (2006).
[25] J. Cleymans, H. Oeschler, K. Redlich, and S. Wheaton, Phys. Rev. C **73**, 034905 (2006).
[26] F. Becattini, J. Manninen, and M. Gaździcki, Phys. Rev. C **73**, 044905 (2006).
[27] W. Ehehalt and W. Cassing, Nucl. Phys. **A602**, 449 (1996); W. Cassing and E. L. Bratkovskaya, Phys. Rep. **308**, 65 (1999).
[28] S. A. Bass *et al*., Prog. Part. Nucl. Phys. **41**, 255 (1998); M. Bleicher *et al*., J. Phys. G **25**, 1859 (1999).
[29] H. Weber, E. L. Bratkovskaya, W. Cassing, and H. Stocker, Phys. Rev. C **67**, 014904 (2003); E. L. Bratkovskaya, W. Cassing, and H. Stocker, *ibid.* **67**, 054905 (2003); **69**, 054907 (2004); Prog. Part. Nucl. Phys. **53**, 225 (2004); E. L. Bratkovskaya, S. Soff, H. Stocker, M. vanLeeuwen, and W. Cassing, Phys. Rev. Lett. **92**, 032302 (2004).
[30] M. Asakawa, U. Heinz, and B. Müller, Phys. Rev. Lett. **85**, 2072 (200).
[31] S. Jeon and V. Koch, Phys. Rev. Lett. **85**, 2076 (2000).
[32] E. V. Shuryak and M. A. Stephanov, Phys. Rev. C **63**, 064903 (2001).
[33] B. Mohanty, J. Alam, and T. K. Nayak, Phys. Rev. C **67**, 024904 (2003).
[34] G. Baym and H. Heiselberg, Phys. Lett. **B469**, 7 (1999).
[35] S. Jeon and V. Koch, Phys. Rev. Lett. **83**, 5435 (1999).
[36] C. Roland *et al*. (NA49 Collaboration), J. Phys. G **30**, S1381 (2004).
[37] S. Voloshin, V. Koch, and H. Ritter, Phys. Rev. C **60**, 024901 (1999).
[38] M. Gaździcki and St. Mrówczyński, Z. Phys. C **54**, 127 (1992).
[39] St. Mrówczyński, Phys. Lett. **B439**, 6 (1998).
[40] J. Cleymans and K. Redlich, Phys. Rev. Lett. **81**, 5284 (1998).
[41] S. Wheaton, J. Cleymans, and M. Hauer, Comput. Phys. Commun. **180**, 84 (2009).
[42] S. V. Afanasiev *et al*. (NA49 Collaboration), Phys. Rev. C **66**, 054902 (2002); C. Alt *et al*. (NA49 Collaboration), *ibid*. **77**, 024903 (2008); B. I. Abelev *et al*. (STAR Collaboration), arXiv:0808.2041 [nucl-ex].
[43] St. Mrówczyński, Phys. Lett. **B459**, 13 (1999).
[44] G. Torrieri, Int. J. Mod. Phys. E **16**, 1783 (2007); J. Phys. G **35**, 044009 (2008).
[45] D. Kresan and V. Friese, PoS **C FRNC2006**, 017 (2006).
[46] Z. Ahammed *et al*. (STAR Collaboration), J. Phys. G **35**, S104092 (2008).
[47] B. Zhang, C. M. Ko, B. A. Li, and Z. Lin, Phys. Rev. C **61**, 067901 (2000).
[48] X. N. Wang and M. Gyulassy, Phys. Rev. D **44**, 3501 (1991).
[49] M. A. Stephanov, arXiv:0809.3450 [hep-ph].